JOURNAL OF CATALYSIS 114, 447–456 (1988)

Direct Alcohol Synthesis Using Copper/Cobalt Catalysts

W. X. PAN,[1] R. CAO,[2] AND GREGORY L. GRIFFIN

Department of Chemical Engineering, Louisiana State University, Baton Rouge, Louisiana 70803

Received March 7, 1988; revised June 8, 1988

We have measured the yields of methanol, higher alcohols, and hydrocarbons during CO hydrogenation on a $Cu/Co/ZnO/Al_2O_3/K$ catalyst. The overall yield of higher alcohols increases linearly with CO conversion, and the individual higher alcohol yields obey a Schulz–Flory distribution through n-$C_6H_{13}OH$. The selectivity for hydrocarbon products also increases with CO conversion. The product alcohols do not undergo a significant degree of secondary reaction at the concentrations formed under these conditions. The overall results are consistent with a mechanism for higher alcohol synthesis that involves chain growth of a common surface alkyl intermediate, followed by a chain termination step which determines whether the final product desorbs as an alcohol or hydrocarbon. The selectivity of the termination step shifts toward greater hydrocarbon formation with increasing CO conversion.

INTRODUCTION

The phase-out of lead-containing antiknock compounds from motor fuels is causing refiners to look for alternate methods to enhance octane ratings. One approach being explored is the addition of oxygenates such as alcohols or ethers as gasoline blending agents. The potential volume of this market has led to renewed interest in the manufacture of methanol and higher alcohols via synthesis gas derived from coal or natural gas (*1, 2*).

Several catalysts have been studied for this reaction. These include alkalinized Cu/ZnO (*3, 4*), sulfided Mo/Al_2O_3 (*5, 6*), supported Rh or Pd promoted by any of several transition metals (*7–11*), and supported Co alloyed with a second transition metal (*12–15*). The product distribution for the modified Cu/ZnO catalysts includes large amounts of ethanol, propanol, and isobutanol, which suggests that the chain growth mechanism involves a heterogeneously catalyzed analog of the aldol condensation reaction (*16*). In contrast, the other three types of catalyst yield a Schulz–Flory distribution of C_2–C_6^+ alcohols, which suggests that the growth mechanism is similar to that of the Fischer–Tropsch reaction (*9*).

Most of the mechanistic studies of the higher alcohol synthesis on catalysts which yield Fischer–Tropsch product distributions have involved promoted Rh catalysts. Sachtler has proposed a mechanism which leads to a very concise description of the expected product distribution on the basis of well-known reactions involving surface intermediates (*9*). This mechanism is reproduced in Fig. 1. The individual elementary steps in this model are defined in terms of their selectivity: γ is the fraction of the total converted CO that is directly hydrogenated to produce CH_3OH. $(1 - \gamma)$ is the fraction of converted CO that dissociates first and is then hydrogenated to produce a $CH_{x(a)}$ surface intermediate. α_i is the fraction of $C_{i(a)}$ surface alkyl intermediates that undergo a condensation reaction with a neighboring $CH_{x(a)}$ group to produce the homologous $C_{i+1(a)}$ surface intermediate (i.e., the chain propagation step). β_i is the fraction of $C_{i(a)}$ surface intermediates which undergo CO insertion and subsequent hydrogenation to produce the homologous gas-phase C_{i+1} ox-

[1] Visiting scholar, Department of Chemistry and Chemical Engineering, Tsinghua University, Beijing, PRC.

[2] Visiting scholar, Research Institute, Nanjing Chemical Industry Company, Nanjing, PRC.

0021-9517/88 $3.00

ygenated product. $(1 - \alpha_i - \beta_i)$ is the fraction of $C_{i(a)}$ surface intermediates whose growth is terminated by hydrogenation or dehydrogenation to produce the corresponding gas-phase C_i alkane or alkene.

The rate of formation of each individual product in the overall reaction network can be expressed in terms of the rate of CO conversion, r_{CO}, times a factorial combination of these selectivity parameters. For the products of interest in the present work, these expressions are

Methanol

$$r_{MeOH} = r_{CO}\gamma \tag{1}$$

Higher alcohols

$$r_{C_iOH} = r_{CO}(1 - \gamma)\beta_{i-1}\prod_{j=0}^{i-2}\alpha_j \tag{2}$$

Hydrocarbons

$$r_{C_i} = r_{CO}(1 - \gamma)(1 - \alpha_i - \beta_i)\prod_{j=0}^{i-1}\alpha_j. \tag{3}$$

It remains to be shown whether this model, which was developed for promoted Rh catalysts, can also describe the reaction mechanism on Co-based catalysts.

We are presently studying the Co/Cu/ZnO/Al_2O_3 catalyst system, in part to address this question. Courty and Marcilly have published results concerning the preparation and characterization of this type of catalyst (*17*), its activity and overall product distribution (*12*), and its incorporation in a 7000 bbl/day demonstration plant for higher alcohol synthesis (*1*). Our studies have been focused at the fundamental level, with the goal of understanding how the Co, Cu, and alkali components of the catalyst interact to form the active site, and how reaction conditions influence the rate and selectivity of individual products. The latter topic forms the subject of this paper.

EXPERIMENTAL

A single catalyst composition was studied in this work: $40Al_2O_3/0.5K_2O$ (molar basis). The catalyst was prepared by coprecipitation, using starting solutions of 1.0 *M* aqueous $Cu(NO_3)_2$, $Co(NO_3)_2$, $Zn(NO_3)_2$, and $Al(NO_3)_3$, each of which were acidified with HNO_3 as needed to completely dissolve the metal salt. These solutions were mixed in the proportions needed to obtain the desired cation ratio in the final catalyst and then precipitated using 1.0 *M* Na_2CO_3. The mixed nitrates and Na_2CO_3 solution were added simultaneously into a well-stirred beaker, which causes precipitation to occur under neutral pH conditions. The temperature of the mixture was held at 353 K during the precipitation step.

The resulting precipitate was filtered, washed five times in hot water, dried for 12 h at 383 K, and calcined in air for 12 h at 623 K. The alkalinization step was included at this point, by loading the powder to the incipient wetness point which an aqueous solution of K_2CO_3 at the concentration needed to give the desired K loading in the final catalyst and repeating the drying step. The catalyst was loaded into the reactor and reduced *in situ* using a flowing 5 vol%

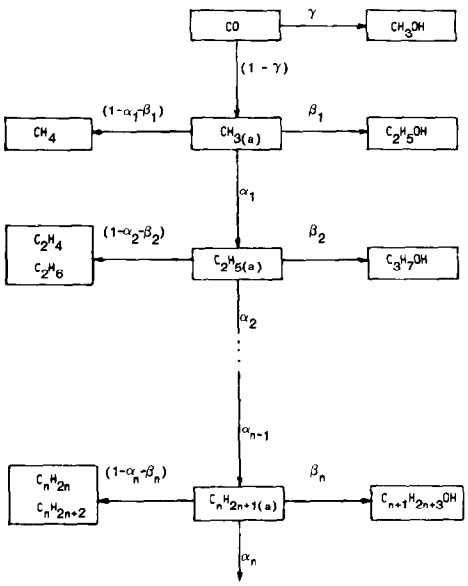

FIG. 1. Proposed mechanism for direct synthesis of higher alcohols on copper/cobalt catalysts.

H_2/N_2 gas mixture at 1 atm. Reduction was performed over 2 days, during which time the temperature was gradually increased to 563 K.

The kinetic measurements were performed in a tubular microreactor. The typical reaction conditions were 50 atm, 563 K, and H_2/CO = 1/1. Products were analyzed by gas chromatography using a Porapak T column with temperature programming and a TCD detector. Peak areas were calibrated by liquid injection of individual components.

RESULTS

In Fig. 2 we show the fractional conversion of CO as a function of reactor space time for the conditions noted above. The space time is defined as W/F = (grams of catalyst)/(moles/hr of inlet CO). The results were obtained by alternatively varying the flow rate between high and low values; this procedure is seen to produce a severe test of the reproducibility of the data. It appears that the results can be reasonably well represented by a straight line through the origin of the graph. This indicates that the rate of CO conversion is approximately constant over the length of the reactor, even when the conversion approaches 80%. The slope of this line, as determined by linear regression, is r_{CO} = 6 (mmol CO)/(g catalyst)(h). This is comparable to the rate of CO conversion reported by Courty *et al.* for their $Cu/Co/ZnO/Al_2O_3/Na$ catalysts (i.e., 9 mmol/g/h, based on data in Ref. (*12*, Table 1).

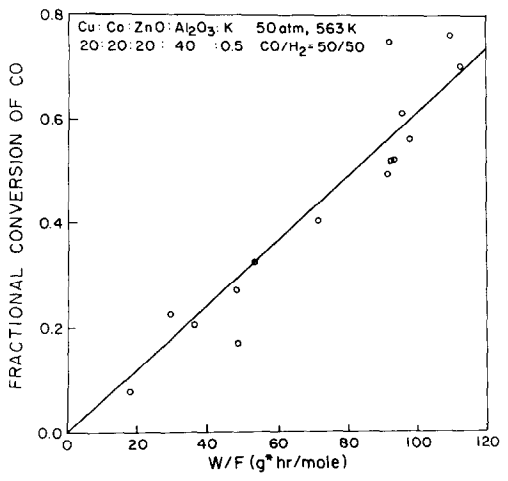

FIG. 2. Fractional conversion of CO as a function of W/F (g catalyst/(mol/h) of inlet CO) on alkali-promoted cobalt/copper catalysts.

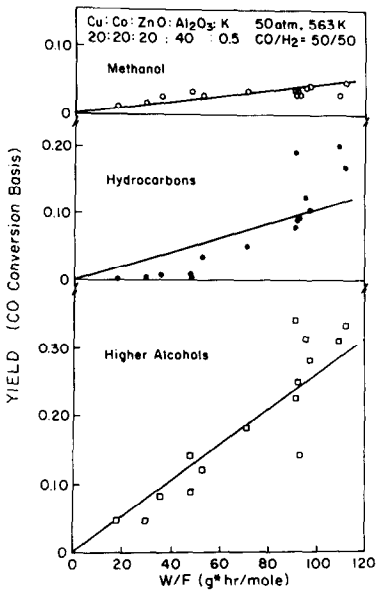

FIG. 3. Yields of CH_3OH, hydrocarbons, and higher alcohols as a function of W/F for alkali-promoted cobalt/copper catalyst. Yields are calculated on the basis of moles of CO converted to each product type.

The yields of methanol, higher alcohols, and hydrocarbons for the same set of measurements are shown in Fig. 3. In this graph we define the yield to be the number of moles of carbon that go into each product classification per mole of CO fed to the reactor (i.e., the fraction of carbon atoms converted to the indicated type of product). This allows the results to be compared directly with Fig. 2, in order to illustrate the molar selectivity of CO conversion into different product types.

The bottom panel shows the fraction of CO converted into higher alcohols (defined here as C_2H_5OH through n-$C_6H_{13}OH$). Again a straight line appears to adequately describe the data. The slope of this line is 3

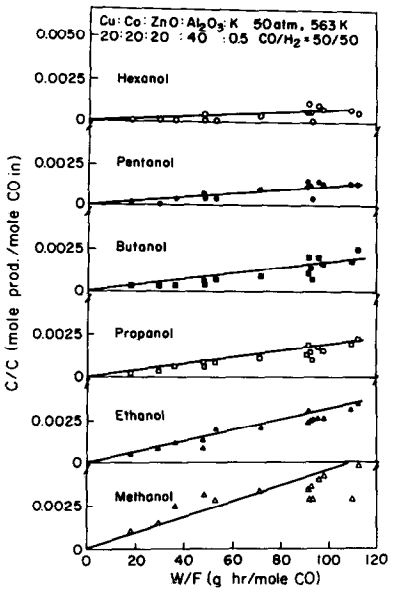

FIG. 4. Yields of individual alcohols as a function of *W/F* for alkali-promoted cobalt/copper catalyst. Yields are calculated on the basis of moles of each product formed.

(mmol CO)/(g catalyst)(h), which represents the molar rate at which CO is being converted into higher alcohol products. Comparing this with the results of Fig. 2, we see that the carbon atom selectivity to higher alcohols is about 50% under these conditions. This is also comparable to the values between 0.46 and 0.49 that can be computed from the results given in Ref. (*12*).

The middle panel shows the fraction of CO converted into hydrocarbons. Unlike the higher alcohol results, these data show a systematic positive curvature. This implies that the rate of hydrocarbon formation increases at higher CO conversions. As discussed below, we believe this is a result of the change in the oxidizing potential of the synthesis gas mixture as the reaction proceeds.

The top panel shows the fraction of CO converted into CH_3OH. This product appears to saturate at high values of *W/F*, which is consistent with an approach to equilibrium conversion under these conditions. The initial slope is 0.5 mmol CO/g catalyst/h, which is much smaller than the rates found on pure CH_3OH synthesis catalysts. The selectivity for CO conversion into CH_3OH is about 8%, which is lower than the value of 20% reported in Ref. (*9*). Thus the present catalyst gives a somewhat larger ratio of higher alcohols to CH_3OH.

Figure 4 shows the yields of individual alcohols as a function of *W/F*. In contrast to Fig. 3, in this graph we define the yield to be the moles of product formed per mole of CO fed to the reactor. This means that the slope of the correlating line in each panel corresponds to the molar rate of formation of that product. Methanol is seen to be the greatest product on a molar basis, with successively smaller yields of each higher alcohol. As noted above, the rate of CH_3OH formation saturates at higher *W/F* values. The rates of formation of C_2H_5OH and *n*-C_3H_7OH appear to be roughly constant. The rates for *n*-C_4H_9OH, *n*-$C_5H_{11}OH$, and *n*-$C_6H_{13}OH$ increase somewhat at higher *W/F* values, in a manner similar to the behavior of the hydrocarbon yields seen in Fig. 3.

The rates of formation of individual products are plotted in Schulz–Flory fashion in Fig. 5. The results for higher alcohols from C_3H_5OH through *n*-$C_6H_{13}OH$ are reason-

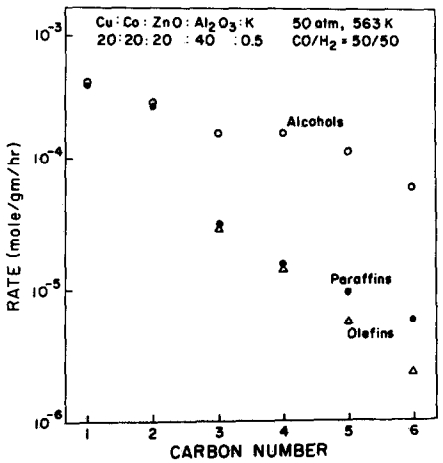

FIG. 5. Schulz–Flory–Anderson plot of product formation rates. Product yields during higher alcohol synthesis.

ably well described by a straight line, which is consistent with the mechanism proposed in Fig. 1. The slope of this line corresponds to a chain propagation factor of $\alpha = 0.71$.

The rate of CH_3OH formation also falls on this line. This is not expected on the basis of the mechanism in Fig. 1, which postulates that CH_3OH is formed independently of the CO insertion reactions that produce all of the higher alcohols. Such a coincidence instead suggests that a single mechanism (e.g., direct homologation) might be responsible for the formation of all alcohols. However, separate experiments described below indicate that this is *not* the case. Instead, the coincidence appears to be the result of a fortuitous choice of reaction conditions.

We have also included the average rates of paraffin and olefin formation in Fig. 5. The slopes for both products differ from those of the alcohol products; the apparent values of the chain propagation factor are $\alpha = 0.44$ for paraffins and $\alpha = 0.37$ for olefins. This is in contrast to the mechanism in Fig. 1, which predicts that all products should have the same propagation factor. The discrepancy may arise because two separate sites with different chain propagation factors might be responsible for alcohol and hydrocarbon products. Alternatively, the fact that the alcohol yields vary linearly with W/F while the hydrocarbon yields show a distinct positive curvature (cf. Fig. 3) suggests that the selectivity of the chain termination step is changing as the reaction proceeds. This could account for the difference in apparent chain propagation factors, without having to invoke the existence of multiple reaction sites.

In Fig. 6 we demonstrate the selectivity of the termination step for the short-chain alcohols C_2H_5OH, n-C_3H_7OH, and n-C_4H_9OH. The ordinate in each panel is defined as the molar yield of the indicated C_{n+1} alcohol, divided by the sum of the molar yields of all other products of length C_n or above. With reference to the mechanism proposed in Fig. 1, this ratio represents the quantity $\beta_n/(1 - \beta_n)$. For all three alcohols, this ratio is near 0.5 for low values of W/F and decreases to between 0.2 and 0.3 as W/F increases. This implies that the values of β_n decrease in parallel from initial values around $\frac{1}{3}$ to final values around $\frac{1}{5}$ over the range of W/F values shown here. Thus it appears that the β_i values are not a strong function of chain length, but they are influenced by changes in reactor conditions brought about by increasing conversion.

One possible cause for these changes is suggested in Fig. 7, where we plot the mole fraction of CO, CO_2, and H_2 leaving the reactor as a function of W/F. We note that the mole fraction values shown here for CO do not correspond exactly to the values of CO conversion shown in Fig. 2, because of the decrease in total mole number as the synthesis reaction proceeds. The mole fractions of CO and H_2 both decrease from 0.5 to around 0.3 over the range of conversions studied, while their ratio remains relatively unchanged from its initial value of 1/1. In contrast, the CO_2 mole fraction increases from 0.0 to 0.2. This change might be ex-

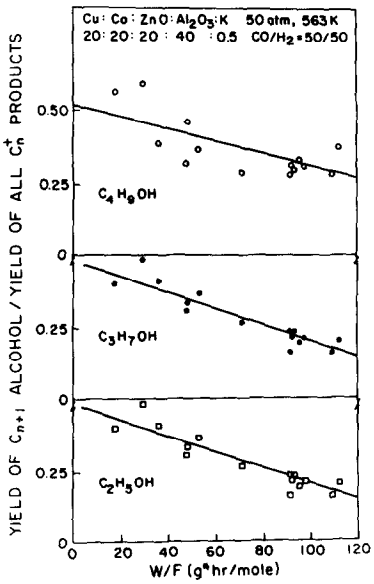

FIG. 6. Selectivity of chain termination step as a function of W/F, shown for C_2H_5OH, n-C_3H_7OH, and n-C_4H_9OH.

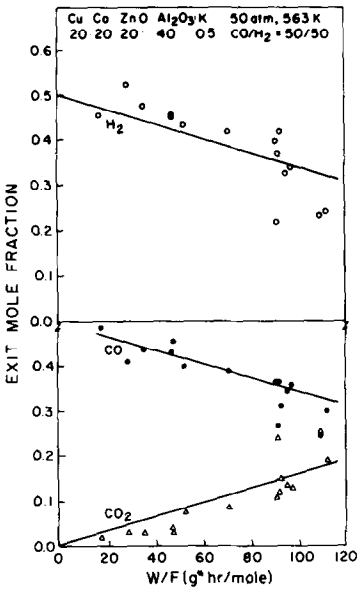

FIG. 7. Reactor concentration profile during high alcohol synthesis. Mole fractions of H_2, CO, and CO_2 leaving the reactor as a function of W/F.

pected to affect the oxidation state of the catalyst surface (see below), which in turn may be responsible for the change in selectivity of the chain termination step.

To test this theory, we performed a transient experiment in which the catalyst was exposed to flowing O_2 for a brief period and then returned to the reaction mixture. The results are shown in Fig. 8, which is a graph of the exit mole fraction of several products as a function of time after returning to the H_2/CO mixture. The oxidation treatment has a pronounced transient effect on the reaction selectivity. The surprising result is that the CH_4 hydrocarbon concentration is increased during the postoxidation transient, while the CH_3OH and C_2H_5OH oxygenate concentrations are decreased.

Similar behavior is observed during start-up, when the catalysts are first exposed to the CO/H_2 mixture after reduction in H_2 alone. Courty and Marcilly (*17*) have noted that the Co component of these catalysts is not completely reduced during the H_2 reduction step, and that further reduction occurs when the CO/H_2 mixture is introduced. Thus we interpret the observed enhancement of hydrocarbon products during start-up as further evidence that changes in catalyst oxidation state are responsible for selectivity changes.

We also decided to test whether an alcohol condensation mechanism might be providing a parallel pathway for chain growth. We did this by connecting a liquid bubbler in series with the inlet stream to the reactor, in order to introduce a saturation pressure of either CH_3OH or C_2H_5OH into the reactant stream. The results for experiments with C_2H_5OH are shown in Table 1.

The first column shows the amount of each alcohol produced under a set of base conditions, i.e., W/F = 32 g-h/mol and no added C_2H_5OH. In particular, we note that the amount of C_2H_5OH measured in the product stream is 0.15 μmol. The next column shows the results when reactant was passed through the bubbler with the temperature adjusted so that the amount of C_2H_5OH measured in the exit stream increased to 1.3 μmol. This level is typical of the largest amount of C_2H_5OH produced without added C_2H_5OH under any reactor conditions (e.g., at the highest values of

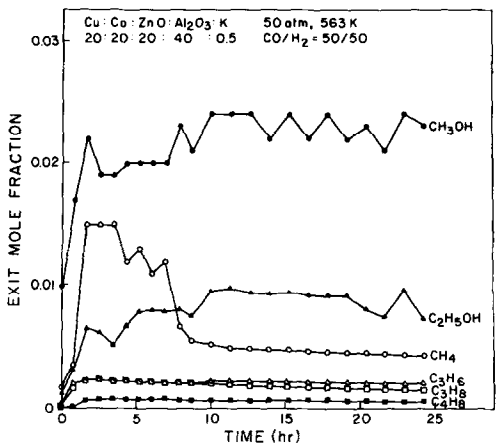

FIG. 8. Influence of preoxidation on product yields. Mole fractions of light products leaving the reactor as a function of time following deliberate oxidation of the catalyst.

TABLE 1

Influence of C_2H_5OH Concentration on Higher Alcohol Yield of $Cu/Co/Zn/Al_2O_3$ Catalysts

	Reactor conditions[a]			
Inlet C_2H_5OH[b]	0.0	1.3[c]	0.0	220
W/F (g-hr/mol CO)	32	24	100	—[d]
	Product amounts[b]			
CH_3OH	0.28	0.25	1.08	0.27
C_2H_5OH	0.15	1.3	1.2	220
C_3H_7OH	0.06	0.08	0.88	15
C_4H_7OH	0.04	0.05	0.96	55
C_5H_9OH	—	—	0.82	2

[a] 563 K, 50 atm, $CO/H_2 = 1.1$

[b] Micromoles measured in GC sampling volume.

[c] Taken as equal to outlet.

[d] *W/F* not determined at this inlet C_2H_5OH concentration.

W/F used in the preceding experiments). It also represents a ninefold increase in the amount of C_2H_5OH present in the reactor, relative to the maximum amount present under the base conditions. In contrast, the amounts of n-C_3H_7OH and n-C_4H_9OH have increased by 30% at most. This shows that the rate of formation of higher alcohols is only weakly affected by the presence of shorter alcohols.

For comparison, in third column we show the alcohol product levels obtained when *W/F* is increased from 30 to 100 without adding C_2H_5OH to the reactant stream. The amount of C_2H_5OH is increased to 1.2 μmol, which is similar to the amount added in the preceding experiment. However, the amount of n-C_3H_7OH and n-C_4H_9OH have both increased more than 10-fold, and a significant amount of n-$C_5H_{11}OH$ is now detected. Clearly, the increase in residence time has a much larger effect on the yield of higher alcohols than does the addition of C_2H_5OH to the inlet stream. Therefore we conclude that the homologation of shorter alcohols does not provide the major pathway for chain growth on this catalyst.

We also tested the effect of using a very high inlet C_2H_5OH concentration. In the last column of Table 1, we list the results obtained when the bubbler temperature was adjusted to produce an C_2H_5OH level of 220 μmol leaving the reactor. This corresponds to a 200-fold increase over the inlet C_2H_5OH concentration used in the experiment of column 2. The largest product change is seen for n-C_4H_9OH, which increases 1000-fold over its value in column 2. The fact that the relative increase in the n-C_4H_9OH product is several times greater than that of the C_2H_5OH reactant shows that the n-C_4H_9OH formation reaction is greater than first order in C_2H_5OH. This suggests that the mechanism for n-C_4H_9OH formation may involve the bimolecular condensation of two C_2H_5OH molecules. A 200-fold increase is observed for the n-C_3H_7OH product amount. This is the same relative increase as that of the inlet C_2H_5OH concentration, which suggests that the n-C_3H_7OH formation reaction is first order in C_2H_5OH. This would be consistent with a mechanism for n-C_3H_7OH formation based on C_2H_5OH homologation. Thus the results in column 4 further confirm that condensation or homologation reactions can become the dominant chain growth pathways, but only at alcohol concentrations much higher than those produced under normal alcohol synthesis conditions.

Similar results are observed when CH_3OH is added to the inlet stream. For example, a 30-fold increase in the inlet CH_3OH concentration causes less than a 2-fold increase in the exit concentration of C_2H_5OH from the reactor. The increase in longer chain alcohols is of similar magnitude.

DISCUSSION

Our present results show that the modified Fischer–Tropsch model for CO hydrogenation proposed by Sachtler for promoted Rh catalysts is also suitable for describing the product distributions obtained on Cu/Co catalysts. We also present evidence to support one modification to the

model, namely that the selectivity ratios for the different chain termination steps are functions of the reaction conditions.

Referring to Fig. 1, the first selectivity parameter, γ, reflects the ratio of converted CO which reacts dissociatively vs nondissociatively. For the present catalyst and reaction conditions, we obtain an apparent value of $\gamma = 0.23$, based on the molar rate of formation of CH_3OH compared to the sum of all other products. This may be compared to the value of $\gamma = 0.065$ reported by Sachtler for $Rh/Mn/Mo/SiO_2$ catalysts (*9*). Additional experiments are needed to determine whether this difference is due primarily to the difference in reaction conditions or catalyst composition. In particular, we can speculate that part of the higher CH_3OH selectivity on the present catalyst may be due to regions of Cu surface area that are not modified by Co.

The next selectivity parameter which appears in Fig. 1 is α, the chain propagation factor. Based on the Schulz–Flory plot given in Fig. 5, we compute a value of $\alpha = 0.7$ for the present reaction. This is significantly larger than the value of $\alpha = 0.4$ reported by Sachtler for the promoted Rh catalyst. It is also higher than the value of $\alpha = 0.45$ reported by Courty *et al.* for *hydrocarbon* products on their $Cu/Co/Al_2O_3$ catalysts (*12*). As we noted when presenting the results in Fig. 5, the hydrocarbon products on our catalyst also have a lower apparent value of α than the majority alcohol products. We attribute at least part of this apparent decrease to changes in the selectivity of the chain termination step as a function of reaction conditions.

The chain termination selectivity factors, β_i, lie between 0.33 and 0.2 in the present work, based on the analysis presented in Fig. 6. These are similar to the values reported for the promoted Rh catalyst; i.e., $\beta_1 = 0.44$, $\beta_2 = 0.36$, and $\beta_3 = 0.21$ (*9*). There are two differences which distinguish the present results: (i) For a fixed value of W/F, the values of β_i are closer together. This implies that the selectivity of the chain termination step is not a strong function of chain length. (ii) All of the β_i values decrease in parallel as a function of W/F. Since CO conversion varies linearly with W/F in these results, this can be interpreted to imply that the β_i values are a function of conversion.

The latter effect may account for the nonlinear dependence of hydrocarbon yields on W/F seen in Fig. 3. We propose that the increase rate of hydrocarbon formation is related to the increase in CO_2 concentration as conversion increases. This presents a paradox, since an increase in the oxidizing potential of the reactant mixture might be expected to favor oxygenate formation. We note at least one precedent for this suggestion, however: Klier *et al.* reported that CH_4 formation increased on a Cu/ZnO catalyst when large amounts of CO_2 are present in the reactant stream (*18*).

In discussing Fig. 6 above, we proposed that the increase in CO_2/CO ratio causes a change in the catalyst oxidation state. Possible reactions include

$$CO_2 + 2\ Cu \Leftrightarrow CO + Cu_2O \qquad (4)$$

$$CO_2 + Co \Leftrightarrow CO + CoO. \qquad (5)$$

The equilibrium constants for the bulk-phase reactants are summarized by Anderson (*19*). For example, the ratio of CO_2/CO required to maintain a stable Cu_2O phase in the presence of metallic Cu at 563 K is 8.5×10^9. The corresponding ratio required to maintain a CoO phase is 4.3×10^3. While these values are both much larger than the maximum CO_2/CO ratio achieved in our reactor, it must be remembered that these calculations are based on the thermodynamics of bulk phase reactions. The equilibrium constants for a surface reaction (i.e., the formation of a single layer of adsorbed oxygen) may be much smaller. For example, Chinchen *et al.* (*20*) have shown that the Cu surface in Cu/ZnO catalysts becomes partially oxidized when exposed to synthesis

gas mixtures that contain a CO_2/CO ratio between 0.25 and 1.8. The relative magnitudes of the equilibrium constants for reactions (4) and (5) suggests that the Co surface is even more likely to be present in an oxidized state.

Catalyst oxidation could also be caused by H_2O produced during the synthesis reaction. The concentration of H_2O observed in the product stream was smaller than the CO_2 concentration. However, the H_2O/CO_2 ratio was larger than the value expected if the water–gas shift reaction were at equilibrium. This means that the effective oxygen pressure due to the H_2O/H_2 couple is greater than that for CO_2/CO. Therefore the calculations based on Eqs. (4) and (5) above are conservative in their estimate of the oxidation potential of the reactant mixture.

The results of adding CH_3OH or C_2H_5OH to the reactant stream show that secondary reactions of alcohol products do not compose the major part of the chain growth mechanism in the present experiments. The condensation reaction which is observed at higher alcohol concentrations appears to be second order in alcohol. This suggests that the mechanism may involve a bimolecular reaction at acid–base sites on the oxide component of the catalyst. The CO insertion reaction involving gas-phase alcohol also occurs at a slower rate than the primary chain growth reaction. This does not rule out CO insertion as the primary chain propagation step in Fig. 1, since the insertion step is postulated to involve a surface alkyl group. Instead, we propose that gas-phase alcohols do not function well as precursors for surface alkyl intermediates. This reflects the difficulty of dissociating the C–O bond in alcohols adsorbed on metal surfaces.

The fact that gas-phase CH_3OH does not cause an increase in chain growth products also appears to eliminate the possibility that the Cu/Co system operates as a bifunctional catalyst, i.e., with CH_3OH being produced on Cu sites and converted to higher products by homologation reactions on Co sites.

SUMMARY

The modified Fisher–Tropsch mechanism proposed by Sachtler to describe the direct synthesis of higher alcohols on promoted Rh catalysts also appears to apply to the $Co/Cu/Zn/Al_2O_3$ catalyst. The selectivity of the chain termination step changes as a function of reaction conditions, with hydrocarbon formation increasing at higher conversion. Future work should focus on determining how these individual rates vary as a function of catalyst composition and reaction conditions.

ACKNOWLEDGMENT

This work was supported by the Department of Energy, Office of Basic Energy Sciences, under Grant DE-FG02-87ER13814.

REFERENCES

1. Courty, Ph., Forestiere, A., Kawata, N., Ohno, T., Raimbault, C., and Yoshimoto, M., *in* "Industrial Chemicals via C1 Processes" (D. R. Fahey, Ed.), ACS Symposium Series No. 328, p. 42. American Chemical Society, Washington, DC, 1987.
2. Haag, W. O., Kuo, J. C., and Wender, I., *Energy* **12,** 689 (1987).
3. Calverly, E. M., and Anderson, R. B., *J. Catal.* **104,** 434 (1987).
4. Vedage, G. A., Himelfarb, P. B., Simmons, G. W., and Klier, K., *in* "Solid State Chemistry in Catalysis" (R. K. Grasselli and J. F. Brazdil, Eds.), ACS Symposium Series No. 279, p. 295. American Chemical Society. Washington, DC, 1985.
5. Dianis, W. P., *Appl. Catal.* **30,** 99 (1987).
6. Klier, K., Santiesteban, J. G., and Nunan, J. G., *Prepr. Amer. Chem. Soc. Div. Pet. Chem.* **32,** 190 (1987).
7. Bhasin, M. M., Bartley, W. J., Ellgen, P. C., and Wilson, T. P., *J. Catal.* **54,** 120 (1978).
8. Katzer, J. R., Sleight, A. W., Gajardo, P., Michel, J. B., Gleason, E. F., and McMillan, S., "Faraday Disc. No. 72," p. 121. Royal Society of Chemistry, 1981.
9. Sachtler, W. M. H., "Proceedings, 8th International Congress on Catalysis, Berlin, 1984," p. I-151. Verlag Chemie, Weinheim, 1984.
10. Ichikawa, M., *in* "Tailored Metal Catalysts" (Y. Iwasawa, Ed.), p. 183. Reidel, Dordrecht, 1986.
11. Kiennemann, A., Breault, R., Hindermann, J. P., and Laurin, M., *J. Chem. Soc. Faraday Trans.* **83,** 2119 (1987).
12. Courty, Ph., Durand, D., Freund, E., and Sugier, A., *J. Mol. Catal.* **17,** 241 (1982).

13. Takeuchi, K., Matsuzaki, T., Arakawa, H., and Sugi, Y., *Appl. Catal.* **18,** 325 (1985).
14. Holy, N. L., and Carey, T. F., Jr., *Appl. Catal.* **19,** 219 (1985).
15. Fujimoto, K., and Oba, T., *Appl. Catal.* **13,** 289 (1985).
16. Natta, G., Colombo, U., and Pasquon, I., in "Catalysis" (P. H. Emmett, Ed.), p. 131. Reinhold, New York, 1957.
17. Courty, Ph., and Marcilly, Ch., in "Preparation of Catalysts" (G. Poncelet, P. Grange, and P. A. Jacobs, Eds.), p. 485. Elsevier, Amsterdam, 1983.
18. Klier, K., Chatikavanij, V., Herman, R. G., and Simmons, G. W., *J. Catal.* **74,** 343 (1982).
19. Anderson, R. B., "The Fischer–Tropsch Synthesis." Academic Press, New York, 1984.
20. Chinchen, G. C., Waugh, K. C., and Whan, D. A., *Appl. Catal.* **25,** 101 (1986).